

Coincidence avoidance principle in surface haptic interpretation

Steven G. Manuel^a, Roberta L. Klatzky^b, Michael A. Peshkin^a, and James Edward Colgate^{a,1}

^aDepartment of Mechanical Engineering, Northwestern University, Evanston, IL 60208; and ^bDepartment of Psychology, Carnegie Mellon University, Pittsburgh, PA 15213

Edited by Dale Purves, Duke University, Durham, NC, and approved January 7, 2015 (received for review July 8, 2014)

When multiple fingertips experience force sensations, how does the brain interpret the combined sensation? In particular, under what conditions are the sensations perceived as separate or, alternatively, as an integrated whole? In this work, we used a custom force-feedback device to display force signals to two fingertips (index finger and thumb) as they traveled along collinear paths. Each finger experienced a pattern of forces that, taken individually, produced illusory virtual bumps, and subjects reported whether they felt zero, one, or two bumps. We varied the spatial separation between these bump-like force-feedback regions, from being much greater than the finger span to nearly exactly the finger span. When the bump spacing was the same as the finger span, subjects tended to report only one bump. We found that the results are consistent with a quantitative model of perception in which the brain selects a structural interpretation of force signals that relies on minimizing coincidence stemming from accidental alignments between fingertips and inferred surface structures.

surface haptic | perception | touch | bumps | kinesthetic

As first demonstrated by Minsky (1) and fully elucidated by Robles-de-la-Torre and Hayward (2), spatial patterns of lateral forces encountered on a flat surface can be perceived as illusory out-of-plane contours. In recent studies using multiple fingers, we have shown that it is possible to modulate single-finger illusions (3) and even to create novel percepts (4). For instance, we have observed that rendering virtual bumps nearly simultaneously on two fingers can induce the percept of a single bump between the fingers (4), an effect we refer to as perceptual collapse (i.e., two bumps collapsing into one as they become simultaneous). Anecdotal evidence suggests that a wider array of effects is possible as well, such as extended contours that span fingers and contours on opposing surfaces that can nullify each other.

We suggest that perceptual collapse is similar to what happens during tool use. When we explore a surface with a tool such as a stylus, we sense coordinated forces at multiple noncontiguous locations on the hand, but the dominant perceptual experience is the action at the tool tip, a phenomenon commonly referred to as distal attribution. It has been proposed that the phenomenal experience of distal effects from proximal stimulation arises from integration of the tool into a self-representation of the body, or body schema (5). Though distal attribution may be descriptive of the perceptual experience of tool use, this construct does not itself provide a theoretical explanation. Our approach, in contrast, attempts to account for virtual bump perception, particularly perceptual collapse, in terms of the cues arising from proximal interaction and the decision processes that operate on those cues. We seek to understand how, given two perceptually viable explanations of the sensory information (two bumps vs. one bump), a single “winning” percept emerges. This explanation should be consistent with an account of the perception of forces from a physical bump explored by the passage of the fingers over it.

A schematic depiction of the collapse effect studied in our experiments is shown in Fig. 1*B*, which depicts forces arising from a virtual tool that couples the fingers. Fig. 1*A* shows the physical forces and Fig. 1*C* a literal interpretation that precludes

collapse. Although our experiment provides no visual cues suggesting that the sensations arise from a single physical entity, which would support collapse, and there are no internal constraint forces that would potentially arise from a tool of the sort shown in Fig. 1*B*, the forces that we display to the fingertips are otherwise consistent with the presence of an intervening tool; in particular, they are temporally synchronized.

Coincidence Avoidance

The explanation for perceptual collapse that we will consider here is that it follows the coincidence avoidance principle. The term was coined by Irvin Rock (6) to describe a hypothesis for solving the structural indeterminacy of visual images. This indeterminacy results from the fact that given a 2D projection of a 3D scene, there are potentially an infinite number of 3D structures that would produce the 2D image (Fig. 2). Coincidence avoidance follows logically from Helmholtz’s general theory of unconscious inference, which proposed that the brain resolves ambiguity using prior knowledge of structures in the world and how those structures translate into visual stimuli (7).

Rock’s hypothesis was that the brain avoids structural solutions that depend heavily on coincidences of viewpoint or arrangement of items in the scene. For example, if we see a shape such as in Fig. 3*A*, we tend to interpret it as a square rather than a cube (Fig. 3*B*) rotated to be viewed face-on; this is because of all of the possible orientations of that cube, very few would result in something qualitatively similar to Fig. 3*A*. In other words, the cube interpretation relies on a highly coincidental orientation. The same is not true for the square interpretation, which for comparatively greater rotations will appear qualitatively similar to the image in Fig. 3*A* (e.g., a single surface with four roughly parallel sides).

When extended to the current situation where one or more bumps are felt by passing the fingers over a surface with a tool, it

Significance

When multiple fingertips experience force sensations during movement, how does the brain decide whether to interpret the forces separately or as an integrated whole? To investigate this question, a force feedback device was used to display forces to two fingertips as they moved collinearly. The force patterns on each finger were constructed to produce illusory virtual bumps, and the distance between these bumps was varied across trials. When bump and finger spacing were identical, subjects tended to report only one bump. This result suggests that the brain selects interpretations of touch sensations that rely on the fewest coincidental alignments between the fingertips and environmental features. This result also has significance for the design of advanced multitouch displays with haptic feedback.

Author contributions: S.G.M., R.L.K., M.A.P., and J.E.C. designed research; S.G.M. performed research; S.G.M., R.L.K., and J.E.C. analyzed data; and S.G.M. wrote the paper.

The authors declare no conflict of interest.

This article is a PNAS Direct Submission.

¹To whom correspondence should be addressed. Email: colgate@northwestern.edu.

This article contains supporting information online at www.pnas.org/lookup/suppl/doi:10.1073/pnas.1412750112/-DCSupplemental.

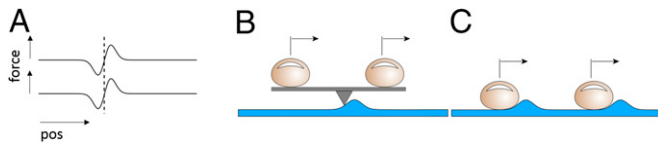


Fig. 1. (A) The force pattern rendered to each finger in the coordinate frames of respective fingers. (B) A schematic representation of a hypothetical tool which allows distal attribution to occur in a surface haptic environment. (C) The more literal interpretation of the force signals as separate bumps under each finger. The surface contours shown in blue represent what is perceived. The actual stimulus rendered to the fingers consists of lateral forces only.

would be a coincidence for two bumps that could appear anywhere along a line to be separated by essentially the same distance as the finger spacing. In contrast, the hypothesis that the same sensations are produced by a single bump does not rely on the same coincidence, because the coupling imposed by the tool will always enforce simultaneity in the two force profiles.

Several investigators have implemented the coincidence avoidance theory using Bayesian models for computer vision problems to identify objects as well as surface characteristics (9–11). To describe the models' function through the square/cube analogy, they essentially determined how well each interpretation (square or cube) would match the visual input (Fig. 3A) for all possible viewpoints. The interpretation that has a better match averaged across all rotations wins the perceptual competition. This particular scenario is consistent with the generic viewpoint principle in human vision, which penalizes interpretations that rely on rare viewing conditions (12) and hence are regarded as coincidences.

Special Case: Causal Inference

Whenever model selection relies on two (or more) separate cues, a judgment must first be made to establish whether the two cues originated from the same cause or two different ones. That is, should the structural hypothesis include one element or two? This judgment is directly applicable to the current work because subjects feel two signals and perceive either one or two causes (bumps).

Multisensory integration implicitly assumes that there is a common cause. For instance, if we estimate the size of an object using visual and haptic cues, we must first assume that what we feel and what we see is the same object or feature. We know that when estimating a parameter like size using multiple sensory cues, the brain tends to combine estimates from each cue, often in a statistically optimal fashion (13); this connects to causal inference because the degree of optimality of that integration has been shown to decrease when the causal linkage between the multiple cues degrades, such as when temporal or spatial discrepancies between cues become too great (14–17). [See Shams and Beierholm (18) for a review of conceptually diverse but mathematically similar approaches to scene parameter estimation in such problems.]

Körding et al. (19) modeled this phenomenon as two steps: causal inference followed by parameter estimation. We used their mathematical framework for the causal inference step to predict the behavior of our collapse effect. The details of the approach can be found in the modeling section below.

Aim of Current Experiment

The current experiment examines the perceptual collapse effect through the lens of coincidence avoidance and specifically the causal inference framework. To accomplish this, we directly manipulated the spatial synchronization of fingers and virtual bumps in a psychophysical task and compared human performance with an ideal Bayesian observer. We used a simplified version of the original demonstration of collapse (4) to limit potential cognitive biases and simplify the analysis.

Materials and Methods

Apparatus. The experimental setup (Fig. 4) consisted of two slider surfaces for two fingertips, constrained to slide along the same linear axis independently of one another. The range of travel for each slider was 70 mm, and their start positions were offset by 60 mm for a combined reachable workspace of 130 mm. Each slider surface was mounted on its own cable-driven linear bearing equipped with load cells to measure both the on-axis (lateral) forces and the vertical (normal) forces exerted by the fingers.

Each slider was driven using a force control loop closed around the slider's lateral direction load cell to mask the mechanism's inertia and friction. The control loop operated at 1 kHz and was computed on a PC/104 stack running an xPC Target real-time operating system. Automation of the experimental protocol was done on a personal computer running a MatLab script that communicated with the PC/104 stack. Visual feedback and user input were accomplished using a touch screen monitor located next to the slider apparatus.

Maxon RE-16 motors drove the sliders with up to 2 N of force, although the experiment required less than 1 N to render bumps effectively. We used Futek LSM250 parallelogram load cells with a full-scale reading of 1.1 N. 320 grit sandpaper was applied to the slider surfaces to ensure zero slip even at low levels of applied normal force.

Lateral forces (representing bumps) were rendered irrespective of the subject's applied normal force; the lateral force applied by the device was a function of slider position alone. We assumed a constant normal force for the purposes of computing lateral force given a desired bump size; this contrasts with an idealized frictionless bump in which lateral force would be proportional to the participant's applied normal force. Because the experiment requires subjects to keep their dominant arm elevated for extended periods, we used a forearm sling to reduce fatigue. The sling's support wires extended 8 feet upward to the ceiling so that the direction of tension during movement was largely insensitive to the position of the arm. In addition, to prevent visual cues from affecting responses, the subject's view of the device was obstructed by a metal sheet.

Participants. The participants included five males and five females between 18 and 25 y of age who gave their informed consent. This research was approved by the Institutional Review Board of Northwestern University. All participants were right-handed, naïve to the purpose of the experiment, and used their dominant hand for the experiment.

Experimental Protocol.

Screening exercise. All subjects went through a screening exercise to ensure their ability to perceive out-of-plane bumps when using the device. Subjects felt several examples of surfaces containing one or two bumps each; their vision of the apparatus was also occluded by a screen for this and the following experimental segments. Subjects were asked to describe the surfaces in terms of number of bumps as well as their heights. As screening criteria, subjects were required to distinguish bump heights that differed by at least 2 mm and detect multiple bumps when they were separated by at least 20 mm.

Subjects were instructed that while traversing over the virtual bumps, they should apply enough pressure on each slider to maintain visually displayed

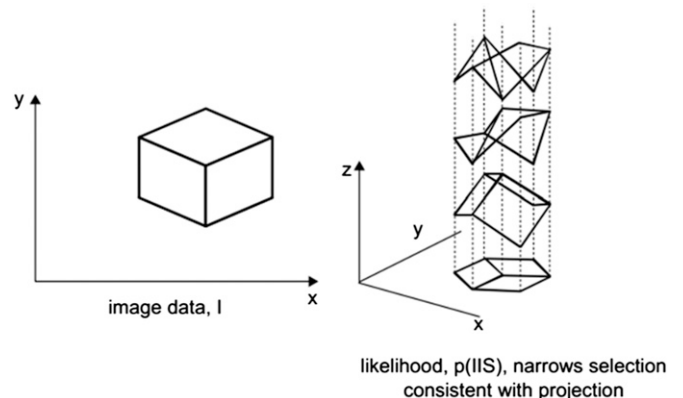


Fig. 2. For a given 2D projection, there are an infinite number of possible corresponding 3D structures. For this reason, visual images are highly structurally indeterminate without the observer having other knowledge about the scene. Reprinted from ref. 8 with permission from Elsevier; www.sciencedirect.com/science/journal/09594388.

pressure indicators, one for each slider, within a target range ($0.5 \text{ N} \pm 0.25 \text{ N}$). Four subjects had to be rejected due to inability to regulate finger pressure or to detect widely spaced bumps as discrete events.

Interbump size equalization. We have observed in previous studies that bumps presented to the thumb are often perceived to be smaller than those for the index finger. We do not currently have a formal explanation for this phenomenon but are able to calibrate the amplitudes of the two bumps to make them perceptually similar. Using the method of adjustment, subjects manually adjusted the amplitude of a bump displayed only to the thumb so that it matched the perceived amplitude of a bump displayed only to the index finger. The measurement was conducted twice to account for asymmetries when approaching the threshold from the top vs. bottom. Using the touch screen, subjects adjusted the thumb bump's amplitude in steps of 0.15 mm from a 4.5- or 8.5-mm initial amplitude, respectively, until it felt subjectively equivalent to the 6 mm tall index finger's bump.

The average of the two final thumb bump amplitudes was used for bumps displayed to the thumb for all following experiments for the given subject. The fixed amplitude used for the index finger was also held constant for future stimulations.

Main experimental procedure. Subjects were told to place their right thumb and index fingers on the two sliders using an open pinch posture (Fig. 4). They were instructed to space their two fingers roughly 60 mm apart and were shown what that spacing looked like. To begin each trial, both sliders had to be positioned at the left side of the workspace 60 mm apart and the finger pressure applied to each had to be within the target range ($0.5 \pm 0.25 \text{ N}$).

Subjects would then maintain that pose while sliding their fingers along the mechanism's full length (horizontally in the figure) multiple times, feeling a bump with each finger. The interbump spacing was varied from 60 to 90 mm in 5-mm increments. Due to the short travel distance (70 mm), neither finger crossed the opposite finger's bump.

For each of these seven conditions, two single-bump catch trials were included, one trial for the index finger and one for the thumb. This block of nine trials was repeated 30 times for a total of 270 trials. Trials were randomized within blocks and mandatory breaks were provided every 90 trials.

Subjects used a metronome to maintain a constant pace of 1.2 s per pass (one way). After two roundtrip passes, subjects reported the number of perceived bumps (0, 1 or 2) using a touch screen.

Subjects were also given feedback if their pace ($1.2 \text{ s per pass} \pm 0.3 \text{ s per pass}$), finger spacing ($60 \pm 3 \text{ mm}$), or finger pressure ($0.5 \pm 0.25 \text{ N}$) were outside of tolerance. The training period consisted of a minimum of 20 trials and terminated when subjects were able to complete eight trials without receiving feedback.

Modeling. To account for the data, we used a Bayesian causal inference model similar to that of Körding et al. (19). In broad terms, the model considers two competing hypotheses for the structure of the surface: h_1 , the surface contains one bump; h_2 , the surface contains two bumps. The goal of the model is to estimate the relative probabilities of these hypotheses, which then corresponds to the ratio of frequencies at which either h_1 or h_2 is accepted as the perceptual outcome. In either hypothesis, the bumps are assumed to be located with equal probability anywhere within a given search region. Under this assumption, it would be coincidental if the surface structure included two bumps that happened to be at the same spacing as the two fingers exploring the surface. In that situation, h_1 becomes much more likely than h_2 , shifting the perceptual outcome.

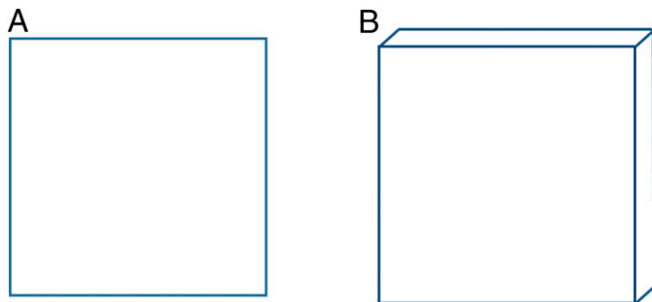


Fig. 3. Upon seeing image A, we tend to imagine a square rather than a cube (B) that has been rotated and viewed face-on. Both interpretations are possible, but the square interpretation is more likely when we consider its robustness to rotation.

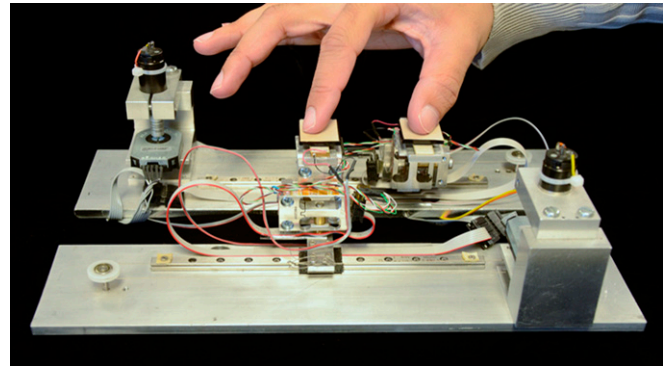


Fig. 4. Experimental apparatus. © 2013 IEEE. Reprinted with permission from ref. 4.

Our goal, therefore, is to compute the probabilities of h_1 and h_2 . We begin by noting that when feeling the virtual surface, the thumb and index fingers sense a pair of bump-like force sensations centered at locations s_1 and s_2 , respectively, both expressed in their respective finger coordinate systems. We distinguish here between force-sensation locations and bump locations because the two will not always be the same depending on the surface hypothesis.

Bayes' theorem can be used to estimate the probability of a hypothesis (h_i) being correct given sensations at s_1 and s as follows:

$$p(h_i | (s_1 \cap s_2)) = \frac{p(s_1 \cap s_2 | h_i) * p(h_i)}{p(s_1 \cap s_2)}, \quad [1]$$

where $p((s_1 \cap s_2) | h_i)$ is the likelihood of feeling sensations at locations s_1 and s_2 assuming the hypothesis h_i is correct. $p(h_i)$ is the prior probability of the i th hypothesis, and $p(s_1 \cap s_2)$ is the joint prior for sensations at both s_1 and s_2 . $p(h_i | (s_1 \cap s_2))$ is known as the posterior probability. Because it is only the ratio of the posteriors for the two hypotheses that is important, and because $p(s_1 \cap s_2)$ will be the same for both one- and two-bump models, we can safely ignore the $p(s_1 \cap s_2)$ term. The prior probabilities of the one- and two-bump hypotheses should be very similar if not identical (i.e., it should not be more or less likely that a surface has one bump rather than two). As a result, $p(h_i)$ is assumed to be the same constant for both hypotheses and can be factored out of the current analysis as well.

Associated with each hypothesis are one or two configuration variables. For instance, in the case of the one-bump hypothesis, the configuration is simply the location c of the bump. In the case of the two-bump hypothesis, the configuration consists of the locations c_1 and c_2 of both bumps (Fig. 5). We also assume the existence of a forward model (9, 19) in the brain that uses a hypothesis h_i and the configuration parameters to generate predicted locations of force sensations felt by the two fingers, x_1 and x_2 (also in finger coordinates to be compatible with s_1 and s_2).

In keeping with the coincidence avoidance principle, because we are interested in how well each hypothesis predicts the sensory data for all plausible configurations on average, we can write the likelihood for the two-bump hypothesis as

$$p((s_1 \cap s_2) | h_i) = \iint p((s_1 \cap s_2) | (x_1(c_1) \cap x_2(c_2))) p(x_1(c_1) \cap x_2(c_2)) dc_1 dc_2, \quad [2]$$

or, equivalently,

$$p((s_1 \cap s_2) | h_i) = \iint p((s_1 \cap s_2) | (x_1(c_1) \cap x_2(c_2))) p(c_1 \cap c_2) dc_1 dc_2. \quad [3]$$

It is important to keep in mind that though the s terms are actual sensed force locations, x and c terms are hypothesized force and hypothesized bump locations, respectively. For the two-bump hypothesis, because x_1 and x_2 are independent of each other and s_1 and s_2 only depend on x_1 and x_2 , respectively, Eq. 3 can be rewritten as

$$p((s_1 \cap s_2) | h_2) = \iint p(s_1 | x_1(c_1)) p(c_1) p(s_2 | x_2(c_2)) p(c_2) dc_1 dc_2 \quad [4]$$

$$p((s_1 \cap s_2) | h_2) = \int p(s_1 | x_1(c_1)) p(c_1) dc_1 \int p(s_2 | x_2(c_2)) p(c_2) dc_2, \quad [5]$$

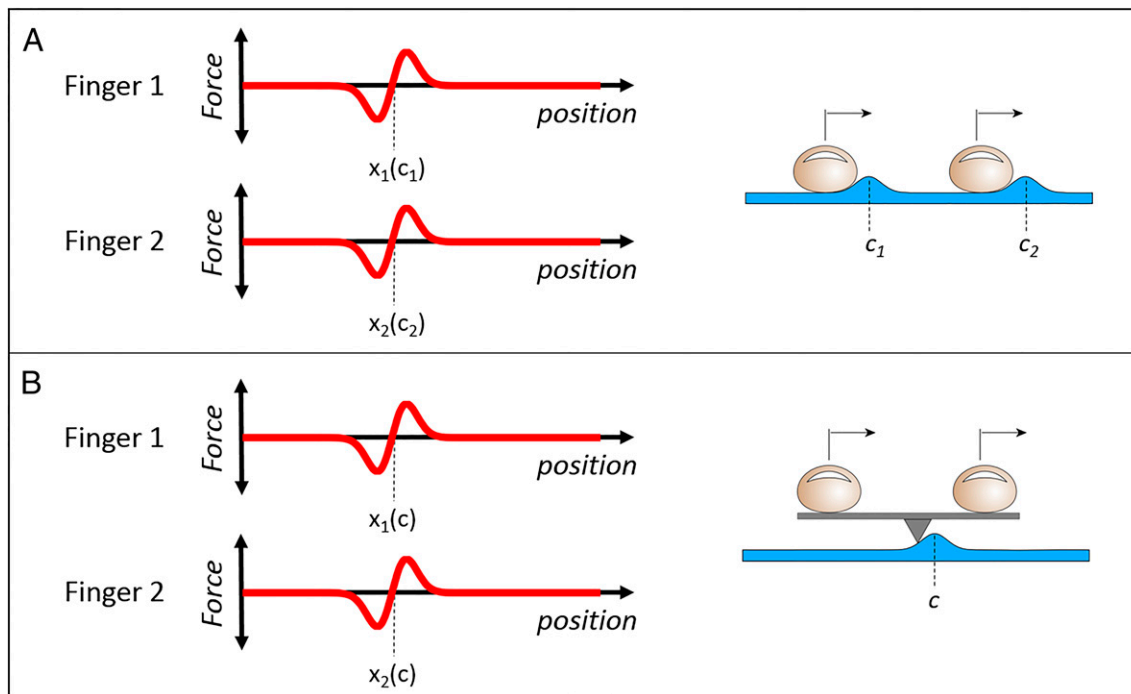


Fig. 5. Expected force sensation locations, x_1 and x_2 , in finger coordinates are a function of the hypothesized bump location(s) in external coordinates. Shown for (A) two-bump and (B) one-bump hypotheses.

where

$$p(s_j|x_j(c_k)) = \frac{1}{\sigma_j \sqrt{2\pi}} e^{-\frac{(s_j - x_j(c_k))^2}{2\sigma_j^2}}, \quad [6]$$

and σ_j is the estimation noise for the location s_j and is equal to the just noticeable difference divided by $\sqrt{2}$. σ_j is the only free parameter in our system that will be fit to the data and assumed to be the same for both fingers in the interest of simplifying the model.

We use a uniform probability density function for c_1 and c_2 over an 85-mm range, centered on the values that correspond to s_1 and s_2 , respectively.

For the one-bump hypothesis, there is only one configuration parameter, c , so its likelihood may be simplified to

$$p((s_1 \cap s_2)|h_1) = \int p(s_1|x_1(c)) p(s_2|x_2(c)) p(c) dc. \quad [7]$$

The distribution of c in this case is also uniform and 85 mm wide. The distribution is centered on a value that results in x_1 and x_2 being symmetrically located about the mean of s_1 and s_2 , so that the prior extends symmetrically over the relevant external sensory area.

Setting $p(c_1)$ and $p(c_2)$ to be uniform distributions does not result in those terms falling out of the analysis because there are two $p(c)$ terms for the two-bump expression (Eq. 5) and only one for the one-bump expression (Eq. 7). This difference in the dimensionality of the feature configuration spaces is what accounts for the difference in coincidence levels associated with the two surface interpretations. In particular, when the force sensations felt by the two fingers occur at locations separated by the same distance as the interfinger separation, the hypothesis that there are two distinct bumps relies on a high level of coincidence.

Results

Manipulation Check. Across subjects, the mean downward pressure applied by the index finger and thumb were 0.67 and 0.68 N, respectively. The corresponding between-subject SDs were 0.14 and 0.12 N. The average rate of motion was 1.15 s per pass with a between-subject SD of 0.04 s per pass.

Actual finger separation tended to fall short of the nominal 60-mm finger separation and also decreased as bumps were

experienced less simultaneously. We found a monotonic decreasing trend of mean finger separation with bump separation [$F(6, 63) = 2.3, P = 0.045$]. Mean finger separations for each bump separation condition ranged from 28.3 to 29.4 mm and are used in later analyses in place of the nominal 30-mm

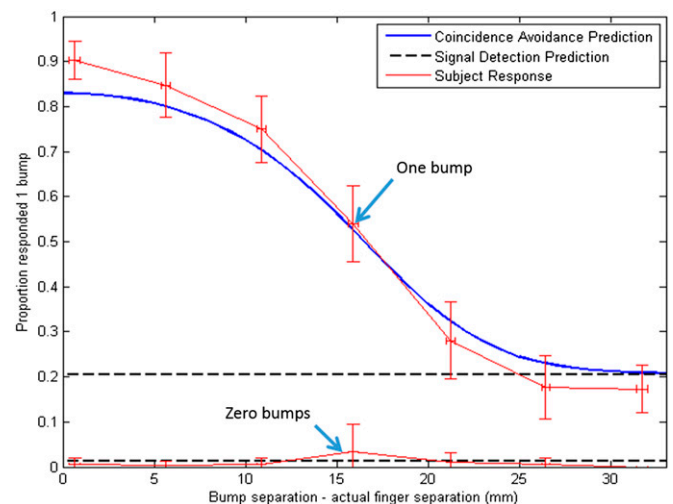


Fig. 6. Predicted vs. reported response rates for number of bumps perceived as a function of the difference between bump separation and finger separation. The dotted black lines show the predicted proportions of trials containing zero (lower line) or one (upper line) detectable bumps, as predicted by detection rates in single-bump catch trials. Red curves denote human subject response rates of zero (lower curve) and one bump (upper curve). The solid blue line is the one-bump response rate predicted by the model, assuming 78% of trials contain two detectable bumps (see text for details). Actual finger separations were averaged across subjects for each nominal finger separation. All horizontal and vertical error bars represent SEs of means.

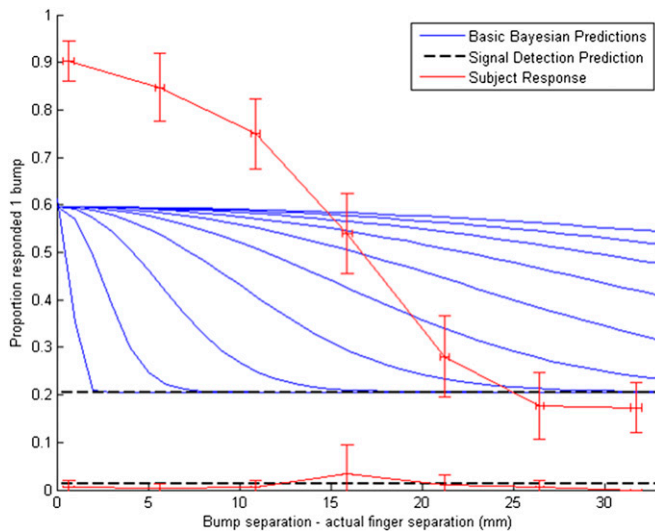


Fig. 7. Comparison Bayesian model without causal inference. All curves are the same as in Fig. 6, except that the solid blue lines are the one-bump response rate predicted by the basic Bayesian model without coincidence avoidance, assuming 78% of trials contain two detectable bumps (see text for details). Each blue curve represents the prediction using a different value of the noise term from 0.3 mm (leftmost) to 3 mm (rightmost) in increments of 0.3 mm. For all values of the noise term, the proportion of one-bump responses when bumps are simultaneous never approaches reported value.

finger spacing. These separation values were measured as the average finger separation when both fingers were in regions where bumps could be rendered (10 mm or more from workspace limits).

Catch Trials. In single-bump catch trials, subjects reported a single bump on average 86.7% of the time and zero bumps 11.7% of the time. A total of 1.6% of catch trials resulted in a two-bump response. For the purpose of establishing a single-bump detection rate, we consider both one-bump and two-bump responses as hits, which gives us a detection rate of 88.3%.

Fitting the Average Response Rates. Fig. 6 shows the averaged responses across all 10 subjects as well as the model's predictions. Based on the catch trial response rates, we assume that 88.3% of bumps are detectable; this means that 78% of two-bump trials should have two detectable bumps, 20.6% should have one, and 1.3% should have none. The model operates on only the 78% that have two detectable bumps. Therefore, if the model-predicted proportion of collapsed bumps for a particular bump separation is C , then the proportion of trials in which subjects report one bump should be $0.206 + 0.78 * C$. The 1.3% predicted zero-bump response rate in the lower red curve of Fig. 6 comes from the catch trial analysis, not the Bayesian model.

The only free parameter in the model is the bump localization noise, σ , which we assume for simplicity to be the same for both fingers. The value of σ that minimizes the sum of squares error between prediction and human subject data are 6 mm. Also, the horizontal axis in Fig. 6 reflects the difference between bump separation and the actual measured finger separations listed in *Manipulation Check*; this gives us the actual discrepancy between bump and finger spacings.

Discussion

Bayesian Model Performance and Alternatives. The model lies within the experimental data's error bounds for all but one data point. When the bump separation and finger separation are nominally the same, the model slightly underpredicts the probability of the collapse effect. One possible explanation is that the bump location just noticeable difference (JND) is not constant but becomes

smaller as bumps become more simultaneous; this is possible because the relevant reference length for making relative location judgments changes with the distance between bumps. When the bumps are nearly simultaneous, they are roughly collocated in finger coordinates, meaning this reference length approaches zero. In that case, we would expect location uncertainty to be limited only by the continuous shape of the bump itself. Future work could involve independently measuring JNDs at various bump separations to test this hypothesis.

Notably, the current model performs far better than a standard Bayesian model, which altogether fails to predict perceptual collapse; to illustrate this, Fig. 7 shows the results of a standard Bayesian model's predictions without the influence of the coincidence avoidance principle. Ten curves are generated for different values of the noise term σ , demonstrating that the predicted rate of reported collapse when bumps are simultaneous (x axis = 0) is fixed at 0.6 and cannot approach the actual rate of 0.9 because the sensations predicted by the one bump felt through a tool and two bumps experienced simultaneously are identical and therefore fit the sensory data equally well. If all bumps were detectable, the predicted rate of collapse would be 0.5 rather than 0.6.

When we fit our model, we assumed an 85 mm width for the uniform probability density function (PDF) of bump location parameter c , based on biomechanical constraints: this width represents a typical range of motion in which one might expect to encounter bumps on a flat surface (see *SI Text* for details). Fig. 8 shows how the width of the PDF can influence the behavior of the model. Some alternative values for width near our assumption (roughly from 75 to 125 mm) yield predictions within 1 SEM of the mean observed value for nonzero abscissa values (as does our model), whereas width values that lead to successful fits near the zero point tend to predict too high a proportion of one-bump responses at larger separations. Thus, though there is some leeway in the assumed PDF width, the original biomechanically motivated value appears to provide a good account of the data.

Catch Trials. It is unclear why 1.6% of single-bump catch trials were interpreted as two bumps. Perhaps because of the mechanical linkage of the thumb and index fingertip through the hand, some faint mechanical effect was present at the opposite

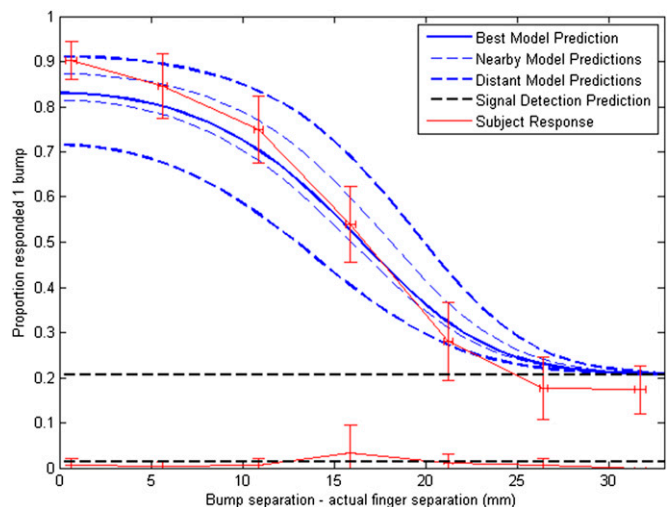


Fig. 8. Coincidence avoidance model predictions for the one-bump response rate using various widths for the uniform probability density function (PDF) of the bump location. The data (red) and fit to the original model (solid blue) are as in Fig. 6. Fits to models with alternative PDF widths are indicated with arrows and numerical values in units of millimeters: bold dashed curves are well beyond 1 SEM of observed data; thin dashed curves lie within most error bounds.

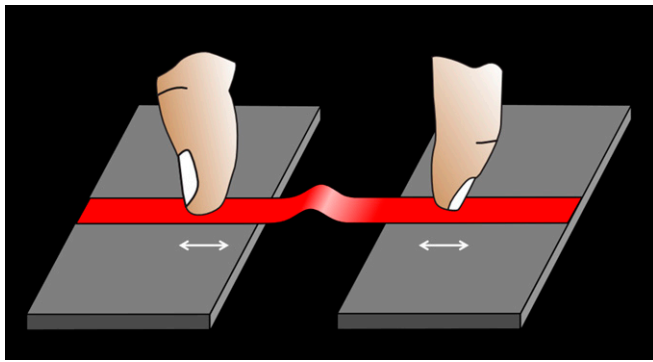


Fig. 9. With the collapsed bump illusion comes the ability to render surface contours between fingers, which may in fact be unreachable by either finger.

finger, which could be interpreted as a second bump. For the purpose of establishing a single-bump detection rate, however, we treated responses of one or two bumps as hits, and zero bumps as a miss.

The 11.7% miss rate could be caused by a number of factors. Drewing (20) observed variation in sensitivity to virtual bumps resulting from exploratory direction. He attributed the effect to the directional dependence of the finger's dynamic mechanical response. In the current experiment, variations in hand posture over time and voluntary cocontraction of opposing muscles could similarly alter the fingers' mechanical response. It is also possible that sensitivity to virtual bumps in general varies somewhat between subjects.

A third explanation is that subjects' criteria in catch trials for what constitutes a nonbump is inherently subjective and could be better regarded as an upper bound for the actual miss rate. Because the right-hand side of the prediction curve in Fig. 6 is exclusively determined by the miss rate, a lower miss rate would allow for a better fit with experimental data.

Conclusion

We have demonstrated that a Bayesian causal inference model is consistent with the behavior of human subjects in reporting whether surface haptic stimuli presented to two fingers originate from one vs. two objective features (virtual bumps). This finding suggests that when there are two plausible interpretations of a sensory event, the brain prefers interpretations that are causally simpler. In these situations, being causally simpler means that

fewer causal parameters must coincide because such coincidences are by definition unlikely in the real world.

We chose to use a fully parametric decision model to best predict the experimental data. However, one limitation of such an approach is that it is restricted to evaluating models that predict stimuli that are parametrically similar to the stimuli used in the experiment. This model could not, for instance, evaluate the likelihood for a model that predicts force profiles of a slightly different shape than those experienced by subjects. Such a mismatch could easily occur in a practical device due to rendering nonidealities. A potential compromise could be a partially parametric approach such as Freeman's (9), which uses an alternative goodness of fit metric between predicted and sensed stimuli. We have found methods like these to be highly flexible in preliminary work and certainly worthy of further study.

Future work is intended to evaluate the Bayesian causal inference model under an expanded range of manipulations. One research direction is to produce different force amplitudes at the two fingers, either directly by rendering or induced by the shape of a tool held in pinch grasp. For example, if one finger explores with greater pressure than the other, its total force vector traces the surface normal of a lower-amplitude bump. The coincidence avoidance model would still produce a one-bump result, but confirming this with additional human subject experiments would help to demonstrate the model's robustness.

It is our hope that others will be able to build on this notion of coincidence avoidance in surface haptics to create design guidelines and possibly real-time control methods for multitouch environments. One might envision, for instance, surface haptic applications where finger trajectories are extrapolated to look ahead for perceptually ambiguous regions. If one is found, features in that region might shift in position such that they trigger the desired perception but are not noticeably out of place. Such a feat would require more general analytical models or heuristics that are highly computationally efficient, but their basis would lie in avoiding or exploiting coincidentally varying sensory inputs.

In addition to controlling higher-order surface interpretations such as perceptual collapse, understanding these illusions also gives us access to novel surface haptic percepts that were previously unknown. This effect in particular allows users of a surface haptic device to explore contours directly, even when they are not in direct contact with the surface and in fact when the surface may not exist (Fig. 9). It is entirely possible that exploitation of the coincidence avoidance principle could enable us to render an even larger class of illusions resulting from different combinations of physical surface geometries and force stimuli.

- Minsky M, Lederman SJ (1996) Simulated haptic textures: Roughness. *Proceedings of the ASME Dynamic Systems and Control Division*, ed Danaï K (Am Soc of Mechanical Engineers, New York), Vol 58, pp 421–426.
- Robles-De-La-Torre G, Hayward V (2001) Force can overcome object geometry in the perception of shape through active touch. *Nature* 412(6845):445–448.
- Manuel SG, Klatzky RL, Peshkin MA, Colgate JE (2012) Surface haptic feature attenuation due to contact on opposing surface. *Haptics Symposium (HAPTICS), 2012 IEEE* (Institute of Electrical and Electronics Engineers, Piscataway, NJ), pp. 31–35.
- Manuel SG, Colgate JE, Peshkin MA, Klatzky RL (2013) Perceptual collapse: The fusion of spatially distinct tactile cues into a single percept. *World Haptics Conference 2013* (Institute of Electrical and Electronics Engineers, Piscataway, NJ), pp. 1–6.
- Holmes NP, Calvert GA, Spence C (2004) Extending or projecting peripersonal space with tools? Multisensory interactions highlight only the distal and proximal ends of tools. *Neurosci Lett* 372(1–2):62–67.
- Rock I (1985) *The Logic of Perception* (MIT Press, Cambridge, MA).
- von Helmholtz H (1867) *Handbuch der Physiologischen Optik* (Voss, Leipzig, Germany); trans Southhall JPC (1962) [*Treatise on Physiological Optics*] (Dover, New York). German.
- Kersten D, Yuille A (2003) Bayesian models of object perception. *Curr Opin Neurobiol* 13(2):150–158.
- Freeman WT (1994) The generic viewpoint assumption in a framework for visual perception. *Nature* 368(6471):542–545.
- Bloj MG, Kersten D, Hurlbert AC (1999) Perception of three-dimensional shape influences colour perception through mutual illumination. *Nature* 402(6764):877–879.
- Liu Z, Knill DC, Kersten D (1995) Object classification for human and ideal observers. *Vision Res* 35(4):549–568.
- Nakayama K, Shimojo S (1992) Experiencing and perceiving visual surfaces. *Science* 257(5075):1357–1363.
- Ernst MO, Banks MS (2002) Humans integrate visual and haptic information in a statistically optimal fashion. *Nature* 415(6870):429–433.
- Roach NW, Heron J, McGraw PV (2006) Resolving multisensory conflict: A strategy for balancing the costs and benefits of audio-visual integration. *Proc R Soc B Biol Sci* 273(1598):2159–2168.
- Slutsky DA, Recanzone GH (2001) Temporal and spatial dependency of the ventriloquism effect. *Neuroreport* 12(1):7–10.
- Parise CV, Spence C, Ernst MO (2012) When correlation implies causation in multisensory integration. *Curr Biol* 22(1):46–49.
- Parise CV, Harrar V, Ernst MO, Spence C (2013) Cross-correlation between auditory and visual signals promotes multisensory integration. *Multisens Res* 26(3):307–316.
- Shams L, Beierholm UR (2010) Causal inference in perception. *Trends Cogn Sci* 14(9):425–432.
- Körding KP, et al. (2007) Causal inference in multisensory perception. *PLoS ONE* 2(9):e943.
- Drewing K (2008) Shape discrimination in active touch: Effects of exploratory direction and their exploitation. *Haptics: Perception, Devices and Scenarios*, ed Ferre M (Springer, Berlin), pp 219–228.

Correction

PSYCHOLOGICAL AND COGNITIVE SCIENCES

Correction for “Coincidence avoidance principle in surface haptic interpretation,” by Steven G. Manuel, Roberta L. Klatzky, Michael A. Peshkin, and James Edward Colgate, which appeared in issue 8, February 24, 2015, of *Proc Natl Acad Sci USA* (112:2605–2610; first published February 9, 2015; 10.1073/pnas.1412750112).

The authors note that the following statement should be added as a new Acknowledgments section: “The authors thank Michael Wiertelwski for contributing the images of fingers and bumps used in this paper. This material is based upon work supported by the National Science Foundation under Grant IIS-0964075.”

www.pnas.org/cgi/doi/10.1073/pnas.1504364112